Insights into the Gluon Propagator: Theory and Phenomenology

Emerson Luna

Universidade Federal do Rio Grande do Sul

Second Latin American Workshop on Electromagnetic Effects in QCD

Santiago, 2025

Outline

- The necessity of nonperturbative corrections:
  - Resummations in QCD
- A solution via QCD effective charges
- Some results
  - Higher twist contributions to F_2
  - Two-gluon exchange model
- Conclusion and Perspectives

Resummations in QCD

■ Some observables can be written, in pQCD, as a power series in α_s

$\Longrightarrow$ in these series the coupling constant is accompanied by large logarithms, which need to be resummed

$\Longrightarrow$ according to the type and to the powers of logarithms that are effectively resummed one gets different evolution equations

■ The solution of the DGLAP equation sums over all orders in α_s the contributions from leading, single, collinear logarithms of the form $\alpha_s \ln\left(Q^2/Q_0^2\right)$

$\Longrightarrow$ it does not include leading, single, soft singularities of the form $\alpha_s \ln(1/x)$, which are treated instead by the BFKL equation

■ The BFKL equation describes the x-evolution of PDFs at fixed Q^2

Resummations in QCD

■ The phase space regions which contribute these logarithms enhancements are associated with configurations in which successive partons have strongly ordered transverse, k_T, or longitudinal, $k_L \equiv x$, momenta:

$$\Rightarrow \alpha_s L_Q \sim 1,\ \alpha_s L_x \ll 1:\ Q^2 \gg k_{T,n}^2 \gg \cdots \gg k_{T,1}^2 \gg Q_0^2$$

$$\Rightarrow \alpha_s L_x \sim 1,\ \alpha_s L_Q \ll 1:\ x \ll x_n \ll \cdots \ll x_1 \ll x_0$$

■ At small-x and low Q^2 (where gluons are dominant) we do not have strongly ordered k_T

$\Rightarrow$ we have to integrate over the full range of k_T

$\Rightarrow$ this leads us to work with the *unintegrated* gluon PDF $\tilde{g}(x, k_T^2)$:

$$xg(x, Q^2) = \int^{Q^2} \frac{dk_T^2}{k_T^2} \tilde{g}(x, k_T^2)$$

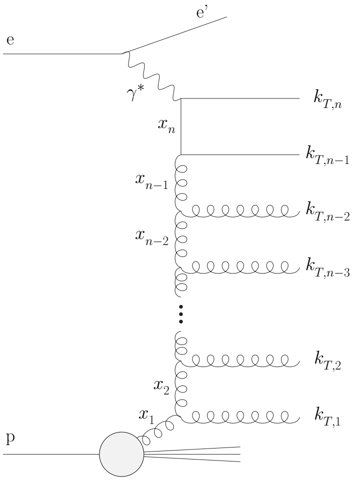

Ladder diagrams

Resummations in QCD

■ The result of resumming these leading terms is sensitive to the infrared k_T region and it is found that

$$\tilde{g}(x, k_T^2) \sim C(k_T^2)\, x^{-\lambda}$$

where $\lambda \sim 0.5$ and $\tilde{g}(x, k_T^2)$ is the *unintegrated* gluon distribution

$\Longrightarrow$ the relation between $\tilde{g}(x, k_T^2)$ and $g(x, Q^2)$, the *standard* gluon distribution reads

$$\tilde{g}(x, k_T^2) = \left. \frac{\partial (xg(x, Q^2))}{\partial \ln Q^2} \right|_{Q^2 = k_T^2}$$

Nonperturbative contributions

- At this point it is clear that nonperturbative contributions are needed:

$\Longrightarrow$ first, the resummation program requires knowledge of the gluon for all k_T^2 including the deep infrared region

$\Longrightarrow$ second, the data in the small-x region show that F_2 tend to a flat shape with decreasing Q^2, particularly for low Q^2

> $\Longrightarrow$ this indicates that the singular behavior $x^{-\lambda}$ predicted by BFKL must be suppressed by nonperturbative effects

- Hence approaching the low Q^2 region from the QCD theory makes evident the problem of how to incorporate in an effective way nonperturbative corrections into the description of some observables

Question: How to address this question?

QCD effective charges

■ The nonperturbative dynamics of QCD may generate an effective momentum-dependent mass $m(q^2)$ for the gluons

□ Numerical simulations indicate that such a dynamical mass does arise when the nonperturbative regime of QCD is probed

$\Longrightarrow$ large-volume lattice QCD simulations, both for SU(2) and SU(3), reveal that the gluon propagator is finite in the deep infrared region

□ In the continuum, it turns out that the nonperturbative dynamics of the gluon propagator is governed by the corresponding Schwinger-Dyson equations (SDEs)

$\Longrightarrow$ according to the SDEs a finite gluon propagator corresponds to a massive gluon

QCD effective charges

■ The QCD effective charge $\bar{\alpha}(q^2)$ is a nonperturbative generalization of the canonical perturbative coupling $\alpha_s(q^2)$

$\Rightarrow$ it is intimately related to the phenomenon of dynamical gluon mass generation

■ The charge $\bar{\alpha}(q^2)$ provides the bridge leading from the deep ultraviolet regime to the deep infrared one

$\Rightarrow$ the definition of $\bar{\alpha}(q^2)$ is not unique: may be obtained in two ways

$\Longrightarrow$ despite the distinct theoretical origins of $\bar{\alpha}(q^2)$, they coincide exactly in the deep infrared.

$\Longrightarrow$ the ultimate reason for this is the existence of a nonperturbative identity relating various of the Green functions appearing in their respective definitions

QCD effective charges

■ For example, $\bar{\alpha}(q^2)$ can be obtained from the Schwinger-Dyson solutions for the gluon self-energy $\hat{\Delta}(q^2)$

$\Rightarrow$ in this definition the solutions for $\hat{\Delta}(q^2)$ are used to form a renormalization-group invariant quantity: $\hat{d}(q^2) = g^2\hat{\Delta}(q^2)$

$\Rightarrow$ the inverse of $\hat{d}(q^2)$ quantity may be written

$$\hat{d}^{-1}(q^2) = \frac{\left[q^2 + m^2(q^2)\right]}{\bar{\alpha}(q^2)}$$

where now

$$\frac{1}{\bar{\alpha}(q^2)} = b_0 \ln\left(\frac{q^2 + m^2(q^2)}{\Lambda^2}\right)$$

QCD effective charges

■ Note that here b_0 is precisely the first coefficient of the QCD β function and Λ is the QCD mass scale

$\Rightarrow$ thus $\bar{\alpha}(q^2)$ has exactly the same form of the leading order (LO) perturbative QCD coupling:

$$\frac{1}{\alpha_s^{LO}(p^2)} = b_0 \ln\left(\frac{p^2}{\Lambda^2}\right)$$

if $q^2 + m^2(q^2) \rightarrow p^2$ in the argument of the logarithm

$\Rightarrow$ this will effectively ensure that, in practice, the QCD effective charge can be successfully obtained by saturating the perturbative strong coupling $\alpha_s^{LO}(q^2)$

QCD effective charges

- That is to say,

$$\bar{\alpha}^{LO}(q^2) = \alpha_s^{LO}(q^2)\Big|_{q^2\to q^2+m^2(q^2)}$$
$$= \frac{1}{b_0 \ln\left(\frac{q^2+m^2(q^2)}{\Lambda^2}\right)},$$

where $b_0 = \beta_0/4\pi = (11C_A - 2n_f)/12\pi$

QCD effective charges

■ A next-to-leading order (NLO) effective charge can be built through the same procedure

$$\bar{\alpha}^{NLO}(q^2) = \frac{1}{b_0 \ln\left(\frac{q^2+4m^2(q^2)}{\Lambda^2}\right)}\left[1 - \frac{b_1}{b_0^2}\frac{\ln\left(\ln\left(\frac{q^2+4m^2(q^2)}{\Lambda^2}\right)\right)}{\ln\left(\frac{q^2+4m^2(q^2)}{\Lambda^2}\right)}\right],$$

where $b_1 = \beta_1/16\pi^2 = [34C_A^2 - n_f(10C_A + 6C_F)]/48\pi^2$

QCD effective charges

■ We investigate three different types of QCD effective charge $\bar{\alpha}^{NLO}(q^2)$

$\Rightarrow$ they can be constructed from two independent dynamical gluon masses having distinct asymptotic behaviors:

$$m_{log}^2(q^2) = m_g^2 \left[\frac{\ln\left(\frac{q^2+\rho m_g^2}{\Lambda^2}\right)}{\ln\left(\frac{\rho m_g^2}{\Lambda^2}\right)} \right]^{-1-\gamma_1}$$

and

$$m_{pl}^2(q^2) = \frac{m_g^4}{q^2 + m_g^2} \left[\frac{\ln\left(\frac{q^2+\rho m_g^2}{\Lambda^2}\right)}{\ln\left(\frac{\rho m_g^2}{\Lambda^2}\right)} \right]^{\gamma_2-1}$$

Curci-Ferrari effective charge

- The first two QCD effective charges can be constructed simply by combining the above equations

- The third effective charge vanishes logarithmically in the infrared, in agreement with some recent lattice results using a renormalization group invariant coupling resulting from a particular combination of the gluon and ghost propagators

$$\bar{\alpha}_{CF}(q^2) = \frac{1}{1 + c_0 \ln\left(1 + \frac{4m_{log}^2(q^2)}{q^2}\right)} \bar{\alpha}_{log}(q^2)$$

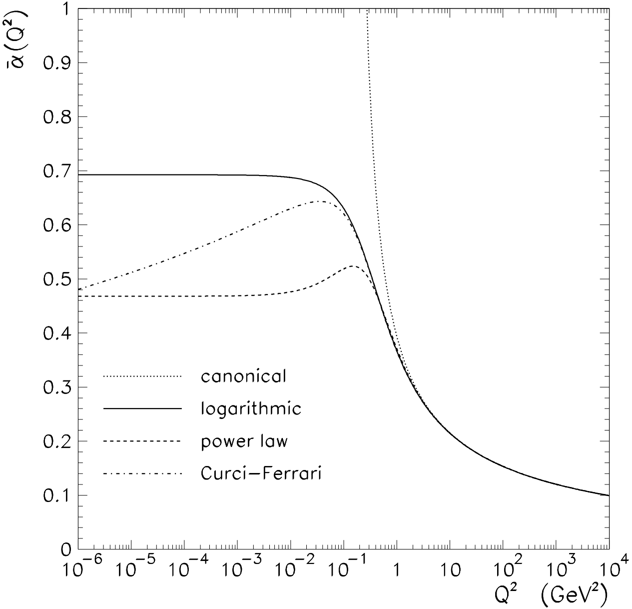

Canonical coupling and QCD effective charges at NLO

Nucleon structure function

■ The nucleon structure function $F_2(x, Q^2)$ at low Q^2 has been measured in the previously unexplored small-x regime at the HERA collider

$\Rightarrow$ a long-standing question is the extent to which the nonperturbative properties of QCD affect the behavior of F_2

$\Rightarrow$ the low Q^2 and small-x regions bring us into a kinematical region where nonperturbative QCD effects becomes essential

These regions are very interesting kinematical domains for testing new QCD theoretical ideas

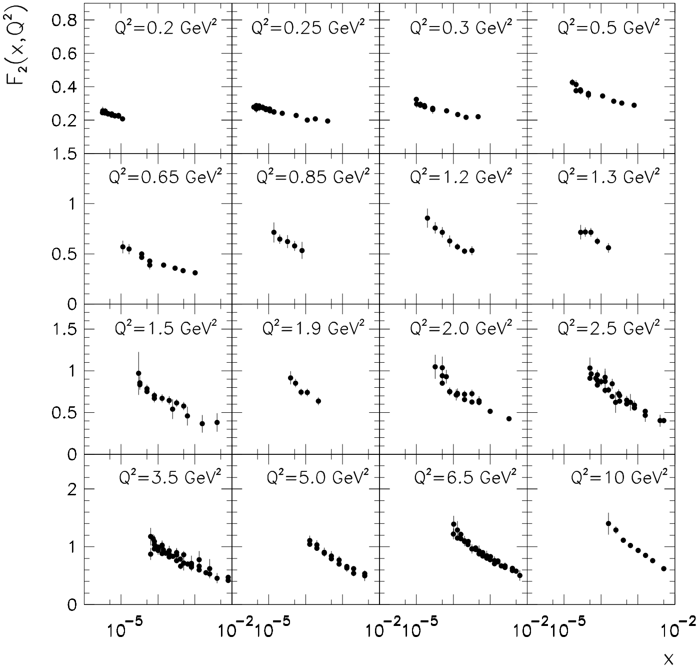
$F_2(x,Q^2)$
Q^2=0.2 GeV^2
Q^2=0.25 GeV^2
Q^2=0.3 GeV^2
Q^2=0.5 GeV^2
Q^2=0.65 GeV^2
Q^2=0.85 GeV^2
Q^2=1.2 GeV^2
Q^2=1.3 GeV^2
Q^2=1.5 GeV^2
Q^2=1.9 GeV^2
Q^2=2.0 GeV^2
Q^2=2.5 GeV^2
Q^2=3.5 GeV^2
Q^2=5.0 GeV^2
Q^2=6.5 GeV^2
Q^2=10 GeV^2
0.8
0.6
0.4
0.2
1.5
1
0.5
0
1.5
1
0.5
0
2
1
0
10^{-5} 10^{-2} 10^{-5} 10^{-2} 10^{-5} 10^{-2} 10^{-5} 10^{-2}
x

Leading-twist expansion of F_2

■ Our task of calculating infrared contributions to the QCD description of data on F_2 can succeed in a consistent way by analyzing exclusively the small-x region

$\Rightarrow$ in this limit some of the existing analytical solutions of the DGLAP equation can be directly used

$\Rightarrow$ in this approach the HERA data at small-x is interpreted in terms of the double-asymptotic-scaling (DAS) phenomenon

$\Rightarrow$ The analytical solutions can be extended in order to include the subasymptotic part of the Q^2 evolution

$\Longrightarrow$ generalized DAS approximation

$\Longrightarrow$ parton distributions evolved from flat x distributions at some starting point Q_0 for the DGLAP evolution

Leading-twist expansion of F_2

- The twist-two term of $F_2(x,Q^2)$ at NLO is given by [1,2]

$$\frac{1}{e}F_2^{\tau 2}(x,Q^2) = f_q^{\tau 2}(x,Q^2) + \frac{4T_R n_f}{3}\,\frac{\alpha_s(Q^2)}{4\pi}\,f_g^{\tau 2}(x,Q^2)$$

$\Rightarrow$ It may be worth emphasizing that this expression is valid only for $x \ll 1$

$\Rightarrow$ The distributions $f_a^{\tau 2}$ are written using a representation which follows from the solution of the DGLAP equation in the Mellin moment space (see [2])

– –

[1]A.Y.Illarionov, A.V.Kotikov, G.Parente, Phys.Part.Nucl.**39**(2008)307;
[2] EGSL, A.L.dos Santos, A.A.Natale, Phys. Lett. B **698** (2011) 52.

Higher-twist corrections

■ In pQCD we make approximations that use the leading power of an expansion in small variables like masses relative to a hard scale Q

⇒ It is natural to ask about the role of non-leading powers

⇒ higher twist corrections to DIS processes have been studied systematically in the framework of the OPE

■ In this scenario the structure functions have *higher-twist* power corrections:

$$F(x, Q^2) = F^{\tau=2}(x, Q^2) + \frac{F^{\tau=4}(x, Q^2)}{Q^2} + \frac{F^{\tau=6}(x, Q^2)}{Q^4} + \ldots$$

Some technical difficulties

■ There are theoretical difficulties of controlling power corrections in effective theories...

$\Longrightarrow$ ... the calculation of power corrections requires the evaluation of the matrix elements of higher-twist operators...

$\Longrightarrow$ ... but in order to cancel certain ambiguities it is also necessary to compute the Wilson coefficient functions to sufficiently high orders of the perturbation series

$\Longrightarrow$ these '*renormalon*' ambiguities are of the same order as the power corrections

■ Fortunately, the twist-4 ambiguity cancels the corresponding ambiguity in the definition of the twist-2 contribution.

The infrared renormalon model

■ Unfortunately, it is not clear if the ambiguity of higher twist contributions can also be canceled

$\Longrightarrow$ in general only a few terms of the perturbative series are known

$\Longrightarrow$ these series are plagued by similar renormalon ambiguities

■ However, the subtle relation between the twist-two and the twist-four contributions has inspired the hypothesis that the main contributions to the matrix elements of the twist-four operators are proportional to their divergent parts

$\Longrightarrow$ this means that in practice we can obtain information about power corrections from the large-order behavior of the corresponding series

$\Longrightarrow$ this approach is called *infrared renormalon model*.

The twist-four ($\tau 4$) correction to $F_2(x, Q^2)$ in the [R]enormalon formalism is given by [3]

$$\begin{aligned} F_2^{[R]\tau 4}(x, Q^2) &= e \sum_{a=q,g} A_a^{\tau 4} \tilde{\mu}_a^{\tau 4}(x, Q^2) \otimes f_a^{\tau 2}(x, Q^2) \\ &= \sum_{a=q,g} F_{2,a}^{[R]\tau 4}(x, Q^2) \end{aligned}$$

$\Rightarrow$ the functions $\tilde{\mu}_a^{\tau 4}(x, Q^2)$ are obtained by means of the infrared renormalon model, and

$$F_2^{[R]}(x, Q^2) = F_2^{\tau 2}(x, Q^2) + \frac{1}{Q^2} F_2^{[R]\tau 4}(x, Q^2)$$

---

[3] D.Hadjimichef, EGSL, M.Peláez, Phys. Lett. B **804** (2020) 135350.

Similarly the twist-six ($\tau 6$) correction to $F_2(x, Q^2)$ reads [3]

$$
\begin{aligned}
F_2^{[R]\tau 6}(x, Q^2) &= e \sum_{a=q,g} A_a^{\tau 6} \tilde{\mu}_a^{\tau 6}(x, Q^2) \otimes f_a^{\tau 2}(x, Q^2) \\
&= \sum_{a=q,g} F_{2,a}^{[R]\tau 6}(x, Q^2)
\end{aligned}
$$

$\Rightarrow$ the functions $\tilde{\mu}_a^{\tau 6}(x, Q^2)$ are also obtained by means of the infrared renormalon model

$\Rightarrow$ now, taking into account all higher twist corrections, we have

$$
F_2^{[R]}(x, Q^2) = F_2^{\tau 2}(x, Q^2) + \frac{1}{Q^2} F_2^{[R]\tau 4}(x, Q^2) + \frac{1}{Q^4} F_2^{[R]\tau 6}(x, Q^2)
$$

- If $F_2^{[R]h\tau}(x,Q^2)$ denotes the higher-twist operators, we have

$$F_2^{[R]}(x,Q^2) = F_2^{\tau 2}(x,Q^2) + F_2^{[R]h\tau}(x,Q^2),$$

where the "+" and the "-" representations of $F_2^{[R]h\tau}(x,Q^2)$ can each be put into a compact form [3]:

$$\begin{aligned}
\frac{1}{e}F_2^{[R]h\tau,+}(x,Q^2) &= \frac{32T_R n_f}{15\beta_0^2}\, f_g^{\tau 2,+}(x,Q^2)\sum_{m=4,6} k_m \Bigg\{ \frac{A_g^{\tau m}}{Q^{(m-2)}}\left(\frac{2}{\rho}\frac{\tilde{I}_1(\rho)}{\tilde{I}_0(\rho)} + \ln\left(\frac{Q^2}{|A_g^{\tau m}|^{l_m}}\right)\right) \\
&+ \frac{4C_F T_R n_f}{3C_A}\frac{A_q^{\tau m}}{Q^{(m-2)}}\Bigg[\left(1-\bar{d}_{+-}^{q}(1)\frac{\alpha_s(Q^2)}{4\pi}\right)\left(\frac{2}{\rho}\frac{\tilde{I}_1(\rho)}{\tilde{I}_0(\rho)} + \ln\left(\frac{Q^2}{|A_q^{\tau m}|^{l_m}}\right)\right) \\
&+ \frac{20C_A}{3}\frac{\alpha_s(Q^2)}{4\pi}\left(\frac{2}{\rho^2}\frac{\tilde{I}_2(\rho)}{\tilde{I}_0(\rho)} + \ln\left(\frac{Q^2}{|A_q^{\tau m}|^{l_m}}\right)\frac{1}{\rho}\frac{\tilde{I}_1(\rho)}{\tilde{I}_0(\rho)}\right)\Bigg]\Bigg\},
\end{aligned}$$

$$\begin{aligned}
\frac{1}{e}F_2^{[R]h\tau,-}(x,Q^2) &= \frac{32T_R n_f}{15\beta_0^2}\, f_g^{\tau 2,-}(x,Q^2)\sum_{m=4,6} k_m \Bigg\{ \frac{A_g^{\tau m}}{Q^{(m-2)}}\ln\left(\frac{Q^2}{x_g^2|A_g^{\tau m}|^{l_m}}\right) \\
&- 2C_A\frac{A_q^{\tau m}}{Q^{(m-2)}}\left[\ln\left(\frac{1}{x_q}\right)\ln\left(\frac{Q^2}{x_q|A_q^{\tau m}|^{l_m}}\right) - p'(\nu_q)\right]\Bigg\},
\end{aligned}$$

with $k_4 = 1$, $k_6 = -8/7$, $l_4 = 1$, and $l_6 = 1/2$.

Results

■ The nucleon structure function $F_2(x, Q^2)$ has been measured in DIS of leptons off nucleons at the HERA collider

$\Rightarrow$ we carry out global fits to small-x $F_2(x, Q^2)$ data at low and moderate Q^2 values

$\Rightarrow$ we use HERA data from the ZEUS and H1 Collaborations, with the statistic and systematic errors added in quadrature

$\Rightarrow$ specifically, we fit to the structure function at $Q^2 = 0.2$, 0.25, 0.3, 0.5, 0.65, 0.85, 1.2, 1.3, 1.5, 1.9, 2.0, 2.5, 3.5, 5.0, 6.5 and 10 GeV^2

■ The global fits were performed using a χ^2 fitting procedure, adopting an interval $\chi^2 - \chi^2_{min}$ corresponding to the projection of the χ^2 hypersurface enclosing 90% of probability

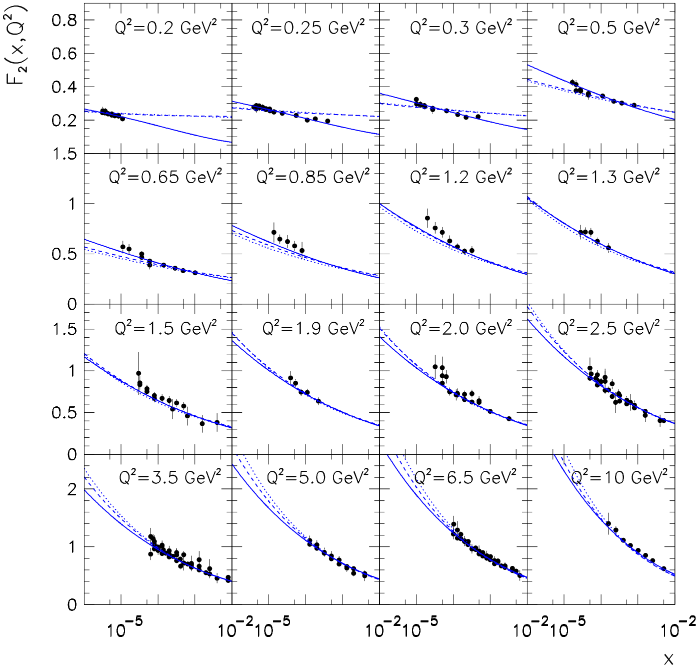
$F_2(x,Q^2)$
Q^2=0.2 GeV^2
Q^2=0.25 GeV^2
Q^2=0.3 GeV^2
Q^2=0.5 GeV^2
Q^2=0.65 GeV^2
Q^2=0.85 GeV^2
Q^2=1.2 GeV^2
Q^2=1.3 GeV^2
Q^2=1.5 GeV^2
Q^2=1.9 GeV^2
Q^2=2.0 GeV^2
Q^2=2.5 GeV^2
Q^2=3.5 GeV^2
Q^2=5.0 GeV^2
Q^2=6.5 GeV^2
Q^2=10 GeV^2
0.8
0.6
0.4
0.2
1.5
1
0.5
0
2
10^{-5}
10^{-2}
x

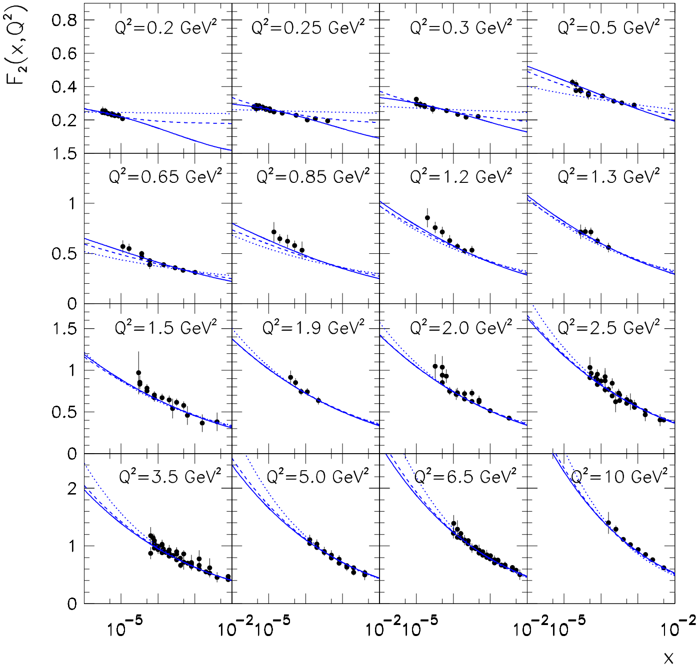
$F_2(x,Q^2)$
Q^2=0.2 GeV^2
Q^2=0.25 GeV^2
Q^2=0.3 GeV^2
Q^2=0.5 GeV^2
Q^2=0.65 GeV^2
Q^2=0.85 GeV^2
Q^2=1.2 GeV^2
Q^2=1.3 GeV^2
Q^2=1.5 GeV^2
Q^2=1.9 GeV^2
Q^2=2.0 GeV^2
Q^2=2.5 GeV^2
Q^2=3.5 GeV^2
Q^2=5.0 GeV^2
Q^2=6.5 GeV^2
Q^2=10 GeV^2
x

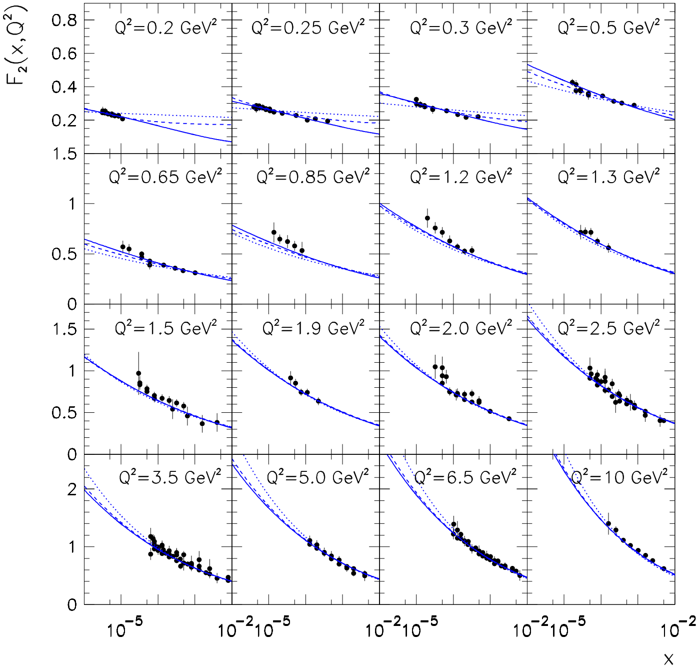
$F_2(x,Q^2)$
Q^2=0.2 GeV^2
Q^2=0.25 GeV^2
Q^2=0.3 GeV^2
Q^2=0.5 GeV^2
Q^2=0.65 GeV^2
Q^2=0.85 GeV^2
Q^2=1.2 GeV^2
Q^2=1.3 GeV^2
Q^2=1.5 GeV^2
Q^2=1.9 GeV^2
Q^2=2.0 GeV^2
Q^2=2.5 GeV^2
Q^2=3.5 GeV^2
Q^2=5.0 GeV^2
Q^2=6.5 GeV^2
Q^2=10 GeV^2
x

Table: The values of the fitting parameters from the global fit to F_2 data. Results obtained using the logarithmic effective charge.

	$\tau 2$	$\tau 2 + \tau 4$	$\tau 2 + \tau 4 + \tau 6$
m_g [MeV]	340±17	284±17	310±53
Q_0^2 [GeV^2]	0.080±0.048	0.54±0.17	0.99±0.16
A_g	0.091±0.070	0.42±0.24	1.19±0.26
A_q	0.727±0.054	0.60±0.12	0.422±0.086
$A_g^{\tau 4}$	-	0.59±0.26	0.58±0.19
$A_q^{\tau 4}$	-	0.020±0.018	0.232±0.081
$A_g^{\tau 6}$	-	-	0.139±0.076
$A_q^{\tau 6}$	-	-	0.0203±0.0082
ν	246	244	242
$\tilde{\chi}$	2.41	2.08	1.21

Table: The values of the fitting parameters from the global fit to F_2 data. Results obtained using the power-law effective charge.

	$\tau 2$	$\tau 2 + \tau 4$	$\tau 2 + \tau 4 + \tau 6$
m_g [MeV]	360±9	282±24	415±67
Q_0^2 [GeV^2]	0.11±0.15	0.929±0.073	1.17±0.19
A_g	-0.090±0.031	0.856±0.080	1.37±0.34
A_q	0.857±0.017	0.488±0.042	0.403±0.081
$A_g^{\tau 4}$	-	0.69±0.14	0.39±0.30
$A_q^{\tau 4}$	-	0.132±0.013	0.38±0.16
$A_g^{\tau 6}$	-	-	0.135±0.073
$A_q^{\tau 6}$	-	-	0.040±0.014
ν	246	244	242
$\tilde{\chi}$	2.88	1.38	1.19

Table: The values of the fitting parameters from the global fit to F_2 data. Results obtained using the Curci-Ferrari effective charge.

	$\tau 2$	$\tau 2 + \tau 4$	$\tau 2 + \tau 4 + \tau 6$
m_g [MeV]	326±72	234±14	302±53
Q_0^2 [GeV^2]	0.05±1.35	0.883±0.071	0.97±0.16
A_g	0.09±0.30	0.846±0.075	1.19±0.28
A_q	0.73±0.31	0.491±0.041	0.420±0.091
$A_g^{\tau 4}$	-	0.65±0.13	0.55±0.19
$A_q^{\tau 4}$	-	0.1179±0.0090	0.224±0.082
$A_g^{\tau 6}$	-	-	0.131±0.076
$A_q^{\tau 6}$	-	-	0.0194±0.0078
ν	246	244	242
$\tilde{\chi}$	2.39	1.34	1.20

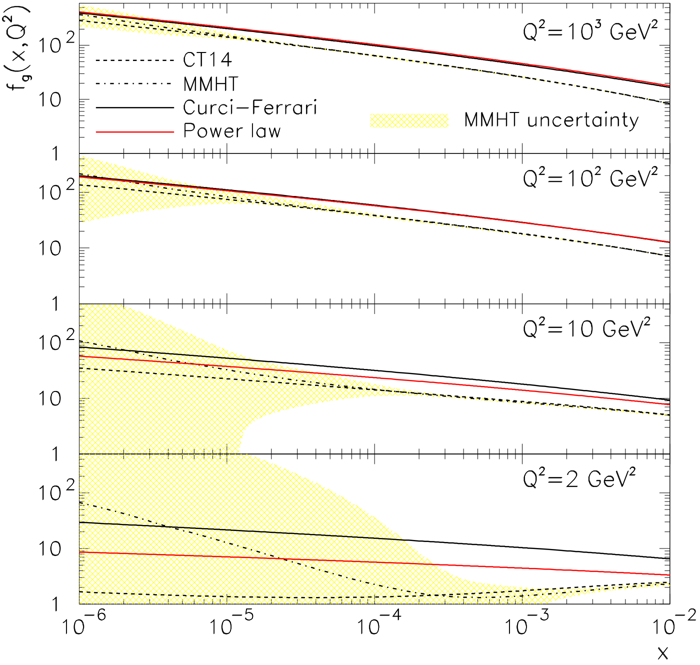

$f_g(x,Q^2)$
$Q^2 = 10^3$ GeV^2
$Q^2 = 10^2$ GeV^2
$Q^2 = 10$ GeV^2
$Q^2 = 2$ GeV^2
CT14
MMHT
Curci−Ferrari
Power law
MMHT uncertainty
1
10
10^2
10^{-6}
10^{-5}
10^{-4}
10^{-3}
10^{-2}
x

The two-gluon-exchange model of the Pomeron

■ It remains a challenge for particle elementary physics to understand the QCD nature of the Pomeron

⇒ various attempts using QCD ideas have been made to study the soft Pomeron

⇒ the lowest-order QCD construction with the correct Pomeron quantum numbers ($C = +1$, color singlet) is the two-gluon exchange

□ In this approach the scattering amplitude is written as:

$$\mathcal{A}(s,t) = is\frac{8}{9}n_p^2\alpha_s^2\,[T_1 - T_2]$$

⇒ T_1 (T_2) represent the contribution when both gluons attach to the same quark (to different quarks) within the proton

The two-gluon-exchange model of the Pomeron

■ The elastic hadron-hadron scattering amplitude through two-gluon exchange is invariably accompanied by a singularity at $-t = 0$

$\Rightarrow$ the origin of this singularity is the pole in the gluon propagator at $-t = 0$

□ Landshoff and Nachtmann (LN) suggested that the gluon propagator is intrinsically modified in the infrared region

$\Rightarrow$ they noticed that the singularity is eliminated if the gluon propagator is finite at $q^2 = 0$

■ Pomeron exchange corresponds to two-gluon exchange in the LN model

The two-gluon-exchange model of the Pomeron

■ The two gluons couple predominantly to the same quark in the hadron, with an amplitude

$$i\beta_0^2\,(\bar{u}\gamma_\mu u)\,(\bar{u}\gamma^\mu u)$$

where β_0 represents the strength of the Pomeron coupling to quarks:

$$\beta_0^2 = \frac{1}{36\pi^2}\int d^2k\,\left[g^2 D(k^2)\right]^2$$

□ The convergence of this integral requires a nonperturbative gluon propagator

□ Very soon after the introduction of these ideas several phenomenological consequences have been discussed in the literature

The two-gluon-exchange model of the Pomeron

■ A LN inspired approach based on the refined Gribov-Zwanziger framework and massive Cornwall-type gluon propagator was used in the calculation of the differential cross sections at LHC [4]

$\Rightarrow$ the calculation provides reasonable description of $d\sigma/dt$ at low energies, namely $\sqrt{s} = 53$ GeV

$\Rightarrow$ the calculation is in complete disagreement with the experimental data at $\sqrt{s} = 7$, 8, and 13 TeV !

□ However, the contribution of the Pomeron component is completely dominant in the LHC regime

$\Rightarrow$ it seems very plausible that any Pomeron-type model should therefore works precisely at the LHC energies

A crucial element is missing...

– –

[4] F.E. Canfora, et al., Phys. Rev. C 96 (2017) 025202.

Reggeization of the scattering amplitude

■ Gluon Reggeization turn out to be of central importance at high energies

□ The gluon Reggeization plays a central role in the derivation of the BFKL equation

⇒ BFKL describes the leading logarithmic evolution of gluon ladders in $\ln s$, in which the vertical lines are Reggeized gluons

⇒ this means that these gluonic lines are not composed of bare gluons whose propagators are given by

$$D_{\mu\nu}(q^2) = -i\frac{g_{\mu\nu}}{q^2}$$

but rather composed of gluons whose propagator is

$$D_{\mu\nu}(\hat{s}, q^2) = -i\frac{g_{\mu\nu}}{q^2}\left(\frac{\hat{s}}{\mathbf{k}^2}\right)^{\epsilon_G(q^2)}$$

Reggeization of the scattering amplitude

$\Rightarrow$ here $\mathbf{k}^2$ is a typical transverse momentum and $\alpha_G(q^2) = 1 + \epsilon_G(q^2)$ is the Regge trajectory of the gluon

■ In the case of color-singlet exchange, a gluon ladder configuration corresponds to a bound state of gluons

$\Rightarrow$ the so called BFKL Pomeron

$\Rightarrow$ by considering the Pomeron Reggeization, one verifies that in the case of the LN Pomeron [5]:

$$\mathcal{A}(s,t) = is^{\alpha_{\mathbb{P}}(t)}\frac{1}{\tilde{s}_0}\frac{8}{9}n_p^2[\tilde{T}_1 - \tilde{T}_2]$$

— —

[5] G.B. Bopsin, EGSL, A.A. Natale, and M. Peláez, Phys. Rev. D **107** (2023) 114011.

Reggeization of the scattering amplitude

where

$$\tilde{T}_1 = \int_0^s d^2k\, \bar{\alpha}\left(\frac{q}{2}+k\right) D\left(\frac{q}{2}+k\right) \bar{\alpha}\left(\frac{q}{2}-k\right) D\left(\frac{q}{2}-k\right) [G_p(q,0)]^2$$

and

$$\tilde{T}_2 = \int_0^s d^2k\, \bar{\alpha}\left(\frac{q}{2}+k\right) D\left(\frac{q}{2}+k\right) \bar{\alpha}\left(\frac{q}{2}-k\right) D\left(\frac{q}{2}-k\right) \times G_p\left(q, k-\frac{q}{2}\right)\left[2G_p(q,0) - G_p\left(q, k-\frac{q}{2}\right)\right]$$

$\Rightarrow \alpha_{\mathbb{P}}(t) = 1 + \epsilon + \alpha'_{\mathbb{P}}$ is the Pomeron trajectory

$\Rightarrow G_p\,(q,k)$ is the convolution of proton wave functions:

$$G_p\,(q,k) = \int d^2p\, d\alpha\, \psi^*(\alpha,p)\, \psi(\alpha, p-k-\alpha q)$$

Nonperturbative gluon propagator

⇒ In this picture $G_p(q,0)$ is simply the proton elastic form factor

⇒ we estimate $G_p\left(q, k-\frac{q}{2}\right)$ assuming a proton wave function peaked at $\alpha = 1/3$ and using

$$G_p\left(q, k-\frac{q}{2}\right) = F_1\left(q^2 + 9\left|k^2 - \frac{q^2}{4}\right|\right)$$

■ The expressions for $\tilde{T}_1$ and $\tilde{T}_2$ include nonperturbative QCD information $\Longrightarrow$ the QCD effective charge $\bar{\alpha}(q^2)$

□ Combining all these results:

$$\frac{1}{\bar{\alpha}_i(q^2)D(q^2)} = b_0\left[q^2 + m_i^2(q^2)\right]\ln\left[\frac{q^2+4m_i^2(q^2)}{\Lambda^2}\right]$$

where $i = log, pl$

Analysis

■ The LHC data requires a more sophisticated version of the convolution of proton wave functions

⇒ This is necessary in order to take account of the fact that the $d\sigma/dt$ data at LHC show a significant deviation from an exponential in the small $|t|$ region

⇒ To obtain a better fit the TOTEM Collaboration have generalized the pure exponential to a cumulant expansion:

$$\frac{d\sigma}{dt}(t) = \left.\frac{d\sigma}{dt}\right|_{t=0} \exp\left(\sum_{n=1}^{N_b} b_n t^n\right)$$

⇒ Here the $N_b = 1$ case corresponds to the pure exponential

Analysis

■ A satisfactory description of the data at $\sqrt{s} = 13$ TeV was achieved in the case $N_b = 3$, with $\chi^2/DoF = 1.22$ and $p - value = 8.0\%$

$\Rightarrow$ TOTEM analyzed data with $|t|_{max} = 0.15$ GeV^2

$\Rightarrow$ This corresponds to the largest interval before $d\sigma/dt$ accelerates its decrease towards the dip region

□ Based on this observed behavior of $d\sigma/dt$, we propose the following convolution of proton wave functions at $k^2 = 0$ (i.e. the form factor):

$$G_p(q, 0) = F_1(q^2) = \exp\left[-\left(\sum_{n=1}^{N_a} a_n |t|^n\right)\right]$$

Analysis

■ The experimental results reveal some tension between the TOTEM and ATLAS measurements of the cross sections

$\Rightarrow$ For example, if we compare the TOTEM result for σ_{tot}^{pp} at $\sqrt{s} = 7$ TeV, $\sigma_{tot}^{pp} = 98.58 \pm 2.23$, with the value measured by ATLAS at the same energy, $\sigma_{tot}^{pp} = 95.35 \pm 1.36$, the difference between the values, assuming that the uncertainties are uncorrelated, corresponds to $1.4\,\sigma$

$\Rightarrow$ If we compare the ATLAS result for the total cross section at $\sqrt{s} = 8$ TeV, $\sigma_{tot}^{pp} = 96.07 \pm 0.92$, with the lowest value measured by TOTEM at the same center-of-mass energy, $\sigma_{tot}^{pp} = 101.5 \pm 2.1$, we see an even more significant difference: $2.6\,\sigma$

■ This strong disagreement clearly indicates the possibility of different scenarios for the rise of the total cross section and consequently for the parameters of the Pomeron

We consider two distinct ensembles of data

Analysis

■ We investigate three cases for the cumulant expansion, namely $N_a = 1$, 2, and 3

⇒ Our philosophy is to adopt the standard statistical χ^2 test in order to evaluate the relativity plausibility of these cases in the light of LHC data

⇒ Specifically, we consider different cumulant cases and the effectiveness of these choices at describing the $d\sigma/dt$ data sets

□ We have first observed that the fit in the case $N_a = 1$ is not supported by either of the two ensembles of data

□ However, the $N_a = 2$ case provides a very good description of the $d\sigma/dt$ data, for both ensembles

⇒ Our model therefore adopt the case $N_a = 2$ for the cumulant expansion. This means that the model has four free parameters: m_g, ϵ, a_1, and a_2

Analysis

Table: The values of the LN Pomeron obtained in fits to $d\sigma^{pp}/dt$ data using the logarithmic dynamical mass $m_{log}(q^2)$.

	Ensemble A	Ensemble T
m_g (GeV)	0.356±0.025	0.380±0.023
ϵ	0.0753±0.0024	0.0892±0.0027
a_1 (GeV^{-2})	1.373±0.017	1.491±0.019
a_2 (GeV^{-4})	2.50±0.53	2.77±0.60
ν	108	328
χ^2/ν	0.71	0.67

Analysis

Table: The values of the LN Pomeron obtained in fits to $d\sigma^{pp}/dt$ data using the power-law dynamical mass $m_{pl}(q^2)$.

	Ensemble A	Ensemble T
m_g (GeV)	0.421±0.030	0.447±0.026
ϵ	0.0753±0.0025	0.0892±0.0027
a_1 (GeV^{-2})	1.517±0.019	1.689±0.021
a_2 (GeV^{-4})	2.05±0.45	1.70±0.51
ν	108	328
χ^2/ν	0.64	0.90

Analysis

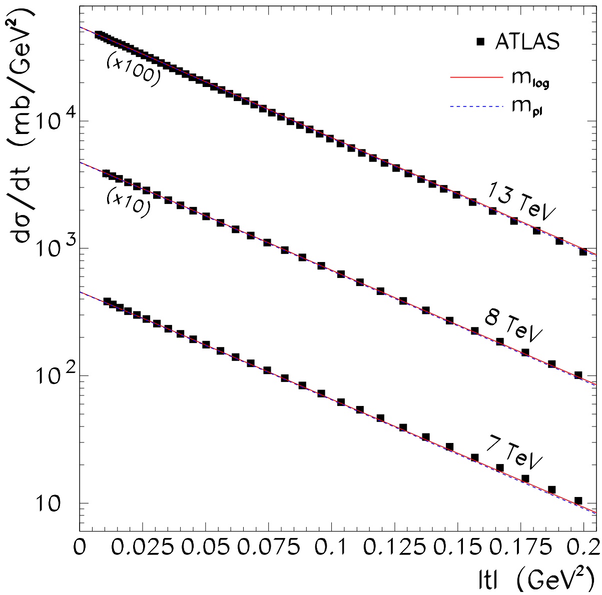

FIG.1: LN Pomeron model description of the *pp* elastic differential cross section data from ATLAS (Ensemble A). The solid and dashed lines show the results obtained using $m_{log}(q^2)$ and $m_{pl}(q^2)$, respectively.

Analysis

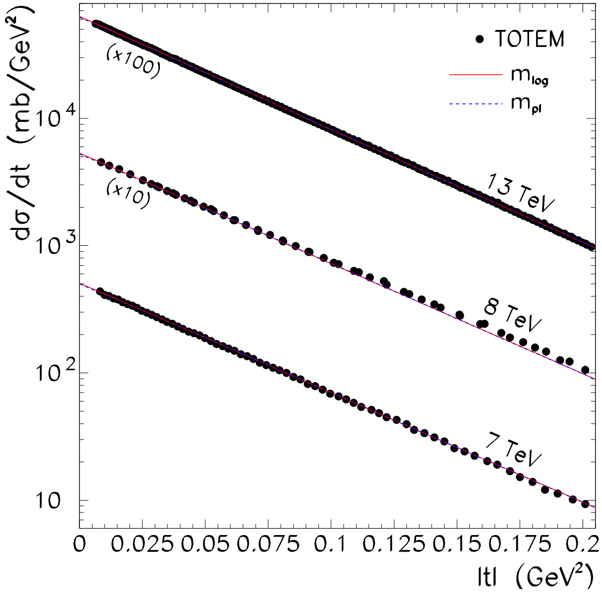

FIG.2: LN Pomeron model description of the *pp* elastic differential cross section data from TOTEM (Ensemble T). The solid and dashed lines show the results obtained using $m_{log}(q^2)$ and $m_{pl}(q^2)$, respectively.

Analysis

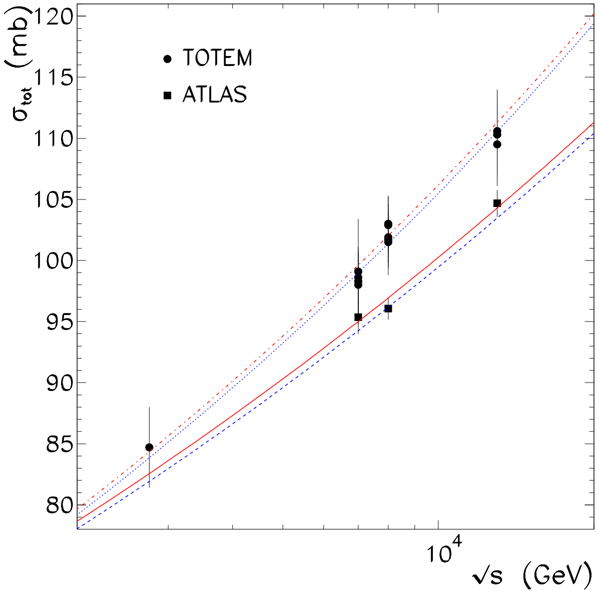

FIG.3: LN Pomeron model prediction for the *pp* total cross section. The solid, dashed, dash-dotted, and dotted lines are the predictions obtained from the fit to Ensemble A using $m_{log}(q^2)$, Ensemble A using $m_{pl}(q^2)$, Ensemble T using $m_{log}(q^2)$, and Ensemble T using $m_{pl}(q^2)$, respectively.

Analysis

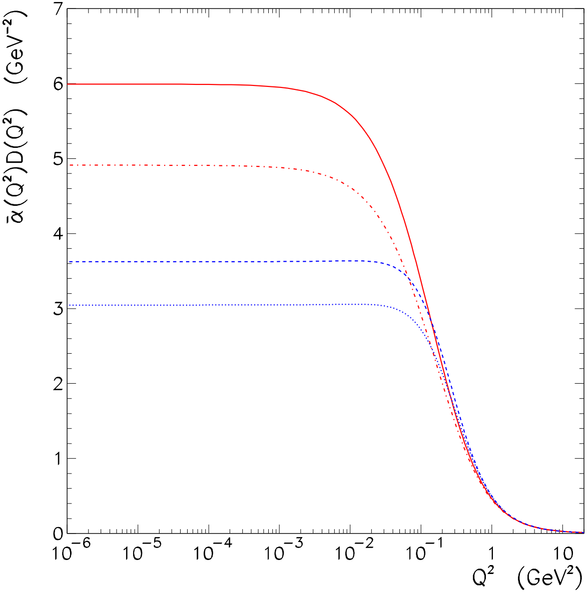

FIG.4: The behavior of the product $\bar{\alpha}_i(q^2)D(q^2)$. The solid, dashed, dash-dotted, and dotted lines are the same as in Figure 3.

Conclusions

■ We have obtained an analytical approach to calculating higher twist corrections to the structure function $F_2(x, Q^2)$

$\Rightarrow$ the formalism is based on existing analytical solutions of the DGLAP equation in the small x region

■ Our analytical approach, when combined with some nonperturbative information from QCD, results in an instrumental tool to study structure functions at very small x region in the infrared regime

■ Comparing the renormalon and standard GDFs, we see that our distributions $f_g(x, Q^2)$ are in good agreement with the CT14 and MMHT ones at very small x

The description of the data requires a nonperturbative gluon propagator

Conclusions

■ We verified that a two-gluon exchange model gives a very good description of the $d\sigma/dt$ data at TeV energies

$\Rightarrow$ provided we demand the Reggeization of the elastic scattering amplitude

$\Rightarrow$ provided we make a suitable choice for the convolution of proton wave functions at $k = 0$

■ We evaluated the relative plausibility of different cumulant expansions for the form factor

$\Rightarrow$ we have described for the first time high-energy differential cross sections data, in the interval $0 < |t| \leq 0.2$ GeV^2, using a LN inspired model

Once again, a nonperturbative gluon propagator is essential for accurately describing the data

Perspectives

■ For inclusive $e^{\pm}p$ DIS process the real experimentally measured data are the reduced cross sections $\tilde{\sigma}$,

$$\frac{d^2\sigma^{e^{\pm}p}}{dx\,dQ^2} = \frac{2\pi\alpha^2 Y_+}{xQ^4}\,\tilde{\sigma}(x, Q^2, y),$$

where $\tilde{\sigma}(x, Q^2, y) = F_2(x, Q^2) - \frac{y^2}{Y_+} F_L(x, Q^2)$, y is the inelasticity, α is the fine structure constant and $Y_+ = 1 + (1 - y)^2$

$\Rightarrow$ F_L is usually treated as a small correction in the F_2 extraction from the reduced cross section $\tilde{\sigma}$

$\Rightarrow$ in our analysis the bias introduced by neglecting F_L is kept to a minimum

Perspectives

$\Rightarrow$ however F_L is an important quantity due to its rather direct relation to $f_g(x, Q^2)$

$\Rightarrow$ thus, it is clearly important to develop a consistent QCD method to describe directly the reduced cross section $\tilde{\sigma}$

$\Longrightarrow$ work in this direction, using the renormalon approach is in progress

Perspectives

■ We plan to extent our analysis to $d\sigma/dt$ data with $|t| > 0.2$ GeV^2

$\Rightarrow$ it is generally believed that at large $|t|$ values the Odderon can play an important role

$\Rightarrow$ in performing calculations in the dip region it is necessary to obtain the real part of the scattering amplitude

$\Rightarrow$ we are developing dispersion relations specially tailored to relate the real and imaginary parts of the LN scattering amplitude

■ We plan to obtain an eikonal version of the LN model

$\Rightarrow$ eikonalization is an effective procedure to take into account some properties of high-energy s-channel unitarity

THANK YOU